Toward steel strip insertion during wire arc additive manufacturing of aluminum alloy smart part

Pascal Robert, Nicolas Beraud, Matthieu Museau, Maxime Limousin, Henri Paris

▶ **To cite this version:**

Pascal Robert, Nicolas Beraud, Matthieu Museau, Maxime Limousin, Henri Paris. Toward steel strip insertion during wire arc additive manufacturing of aluminum alloy smart part. Mechanics & Industry, 2023, 24, pp.15. 10.1051/meca/2023014 . hal-04088547

HAL Id: hal-04088547
https://hal.science/hal-04088547

Submitted on 4 May 2023

HAL is a multi-disciplinary open access archive for the deposit and dissemination of scientific research documents, whether they are published or not. The documents may come from teaching and research institutions in France or abroad, or from public or private research centers.

L'archive ouverte pluridisciplinaire **HAL**, est destinée au dépôt et à la diffusion de documents scientifiques de niveau recherche, publiés ou non, émanant des établissements d'enseignement et de recherche français ou étrangers, des laboratoires publics ou privés.

Mechanics & Industry **24**, 15 (2023)
© P. Robert et al., Published by EDP Sciences 2023
https://doi.org/10.1051/meca/2023014

Mechanics & Industry

Available online at:
www.mechanics-industry.org

REGULAR ARTICLE

OPEN ACCESS

Toward steel strip insertion during wire arc additive manufacturing of aluminum alloy smart part

Pascal Robert*, Nicolas Beraud, Matthieu Museau, Maxime Limousin, and Henri Paris

Univ. Grenoble Alpes, CNRS, Grenoble INP, G-SCOP, 38000 Grenoble, France

Received: 14 December 2022 / Accepted: 28 March 2023

Abstract. Smart parts providing information to the user thanks to an embedded device are an important step toward the industry 4.0. Magneto-strictive properties of steel are well known and thin strips could be embedded in paramagnetic host part to ensure their structural control. Through this study, the feasibility of smarts parts realized by insertion of thin steel strip during aluminum host part manufacturing is more asserted. This study presents a configuration to embed thin steel strip inside massive part realized by Wire Arc Additive Manufacturing (WAAM). This configuration is used to find a correct steel strip − welding torch offset enabling a correct bonding between the deposited bead and the strip without causing any deterioration to the strip. Thickness maps of these strips realized through X-ray tomography allow to evaluate the deterioration of the strips. Scanning electron microscopy is used to evaluate the strength of the bonding through the thickness of the bimetallic interface realized between the steel strip and the aluminum bead. A good bonding between a thin steel strip and a thick part in aluminum alloy thanks to arc welding is obtained. The thickness difference between the two entities welded together represent a ratio of 10, which is 3 times bigger than the previous work reported in literature. Steel to aluminum welding is a challenging research topic and thin to thick element welding as well. This paper address both of these topics together and is a step toward smart metallic part manufacturing.

Keywords: Smart part / aluminum-steel welding / thin to thick welding / tomography / scanning electron microscopy / wire arc additive manufacturing

1 Introduction

Smart parts are a milestone in the upcoming of the industry 4.0 and allows to connect IT technologies and manufacturing technologies. Numerous studies exist to define what a smart part is, and various differences in definitions appears regarding their level of intelligence, their autonomy, their integration or their computing power [1–3]. In this paper, smart parts are defined as parts that provide information to the user or react autonomously when a change in their environment occurs.

They can facilitate several operations such as tracing, customization or structural control. For example, embedding stress sensors during manufacturing of parts can protect the sensors from the hazardous environment where the parts operate and hence facilitate their structural control.

It has been documented that steel is a magnetostrictive material. Its magnetic properties change under stress [4] and can be recorded by induction with a magnetic probe [5]. Steel inserts hence can be used as stress indicators inside metallic host parts if some requirements are met.

Hence the host part must be magnetically invisible (paramagnetic) and the steel insert must not be too deeply embedded below the surface. Furthermore, the steel insert must be very thin in order to be wholly seen by the probe and not just its surface. Hence, the insert will be designated as a strip.

Wire Arc Additive Manufacturing (WAAM) is a process that uses arc-welding technologies to produce part in an additive minded way [6,7]. It enables an easy insertion during the manufacturing process of metal parts. This process can be easily stopped and the manufacturing chamber is easily accessible. Moreover, due to its additive aspects, it is possible to build the part around the steel insert. Hence it appears as a pertinent technology to create metallic smart parts in such a way.

The part made with WAAM technology shall be realized in a paramagnetic and metallic material such as aluminum alloy. Furthermore, the literature in aluminum alloy parts made by WAAM is well developed [8–11]. Moreover, the part has to be massive. A part is made of consecutive layers stacked upon each other and in massive parts, each layer is made of at least two weld beads deposited next to each other. WAAM is a technology that can do this kind of parts. Thus, it shall be possible to

* e-mail: pascal.robert@grenoble-inp.fr

This is an Open Access article distributed under the terms of the Creative Commons Attribution License (https://creativecommons.org/licenses/by/4.0), which permits unrestricted use, distribution, and reproduction in any medium, provided the original work is properly cited.

Table 1. 4043 aluminum alloy wire chemical composition.

Elements	Si	Mn	Cu	Fe	Ti	Zn	Al
Concentration (wt-%)	5.00	0.01	0.02	0.14	0.01	0.01	Bal.

monitor the stress state of WAAM massive aluminum alloy parts with a steel strip embedded between two consecutive beads of several layers.

To ensure the feasibility of such smart parts, the insert must not be deteriorated during the embedding operation. Furthermore, the bonding between the host part and the steel strip insert must present good mechanical properties in order to convey truthfully to the insert, the host part stress state that is monitored.

Obtaining a good bonding between steel and aluminum through an arc-based heat source for additive manufacturing is a complex task. This can be explained by their very different thermo-physics properties. Solid-state solubility of iron in aluminum is indeed very low [12]. Moreover, the arc welding process must not deteriorate the steel strip and has to provide a good bonding between the steel insert and the massive aluminum alloy part. It's a complex task because the welding conditions can be too energetic for the steel strip and deteriorate it and not enough energetic for the thick part and thus not ensure a good bonding between it and the bead produced.

Both of those requirements are complex tasks that need to be answered together in order to show the feasibility of realizing smart parts in this way. The biggest difference of thickness in steel-aluminum welding reported in the literature and known by the author is a 2 mm thick aluminum alloy plate welded to a 0.7 mm thick steel plate in a butt welding configuration [13].

A study to show that it is possible to embed a steel strip in a thick aluminum alloy part and thus prove the feasibility of such smart parts is presented in this paper.

The scope and method followed to prove the feasibility of steel strip embedding in an aluminum alloy host part is first presented. Then, the experimental setup is depicted. The results obtained through tomography and Scanning Electron Microscopy (SEM) are analyzed and finally discussed.

2 Methods

To weld together a thick and thin element without deteriorating the thin element, various best practices can be observed. One of them consist in using a heat sink on the thinner element to help its heat evacuation [14]. Another one consists in selecting an appropriate welding technology to reduce the heat input. A welding technology using the feed wire as the positive electrode is advised [15]. Cold Metal Transfer (CMT) technology has demonstrated its capability in welding thin element together [16]. Furthermore variations of this welding technology using inversions of polarity between the part and the wire feed lead to lower heat input.

Welding together a steel part and an aluminum alloy part is equally a difficult task.

The strength of the bonding obtained through welding is defined by the nature and the thickness of the bimetallic layer that should be created between steel and aluminum. This bimetallic layer is composed of Fe2Al5 and FeAl3 [17,18]. Literature shows that high mechanical resistance is obtained when this layer is thinner than 10 µm [19].

To control the thickness of this layer, different issues must be addressed:
– Steel coating composition.
– Alloying elements in the aluminum alloy selected.
– Welding parameters.
– Torch position.

To improve the wettability of aluminum on steel, and hence their bonding capability, a coating can be applied on steel. A zinc coating is hence selected [18].

An AlSi5 aluminum alloy is equally selected [20] to improve the strength of the bonding.

In the same objective, torch welding parameters have been selected to minimize heat input [21] and being suitable to create a wetted bead with a massive part.

In the following section, different torch-strip distances (offset) are investigated.

All the experimentations are done with a welding robot equipped with a CMT welding torch linked to a TPS4000 Advanced welding station. The substrate selected is a 5mm thick plate of a 5083 aluminum alloy. A 4043 ESAB aluminum alloy wire of 1.2 mm of diameter is used. Its composition is detailed Table 1. The wire diameter is selected to produce a bead suitable to create a massive part by WAAM.

A CMT Pulse Advanced (CMT-PADV) synergic law is recommended by literature to produce WAAM aluminum alloy part with low porosity with CMT technology [22]. This law use polarity inversion between positive polarity welding cycles and negative polarity welding cycles [23]. Thus, a CMT-PADV synergic law is selected.

A heating device is used to preheat the plate and to favor wetting of the deposited bead on the plate [24].

To evaluate the steel strip deterioration after the bead deposition, x-ray tomography shall be used. It can provide a three-dimensional topography of the steel strip without being impaired by the covering aluminum bead deposited.

The bonding quality can be evaluated by inspecting the steel aluminum interface thanks to Scanning Electron Microscopy (SEM). Indeed, a tensile test could be done to assess these results but analysis through SEM represented a lesser risk of error. The tensile testing needed a particular attention to the setup due to the difference of geometry between both sides of the samples that could lead to great error due to clamping jaw micro-misalignment in the tensile machine. Furthermore, the composition of this interface can be determined by Energy Dispersive X-ray

Table 2. DX51D steel strip chemical composition.

Elements	C	Si	Mn	P	S	Ti	Fe
Concentration (wt-%)	0.18	0.50	1.20	0.12	0.045	0.30	Bal.

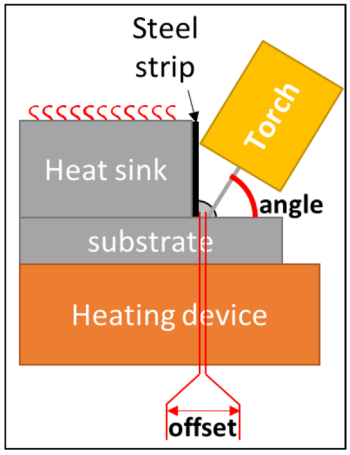

Fig. 1. Experimental set up.

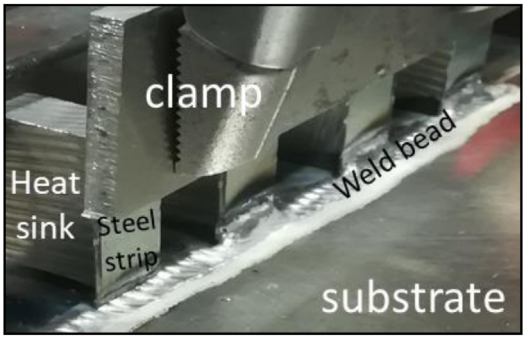

Fig. 2. Pictures of the experimental setup.

Spectroscopy (EDS). Thus, it can be used to ensure the bimetallic layer is present and composed of what is expected by literature.

3 Experimental

Thin steel strips are realized by cutting a 15 mm band of 0.55 mm thick steel foil of DX51D Z100. Its composition is described Table 2.

The steel strips are positioned on the substrate such as presented Figures 1 and 2.

An aluminum alloy block used as a heat sink is positioned behind the steel strip to protect it from deterioration by improving its heat and electrical evacuation. It equally helps positioning vertically the strip on the substrate.

Positioning vertically the strip is necessary to weld on both sides of the steel strip to ensure a symmetric bonding and a faithful stress transfer from the host part to the strip.

The aluminum alloy block shall be less wide than the strip in order to not be welded with it. It has to be removable so as to let the other side of the strip accessible to embed it properly by welding on both sides of the strip.

The deposited bead is realized with the process parameter selected (such as Wire Feed Speed (WFS), Torch Speed (TS) or polarity balance parameter (EP/EN)) which are presented in Table 3. They produce a bead that present dimensions and heat input detailed in Table 4 which is corresponding to the 110-130J/mm range advised by [25] for steel-aluminium alloy welding with CMT-PADV. A torch-working angle of 45° is observed.

A bead is realized in front of each steel strip with different offset from 0.5 mm to 5 mm by step of 0.5 mm.

4 Results

Samples are analyzed in regards to their deterioration and their bonding. Samples realized with an offset below 1.5mm show strips that are deteriorated by the bead deposition as it can be seen in Figure 3. Samples realized with an offset above 3 mm present a bad bonding between the strip and the deposited bead as it can be seen Figure 4.

Samples realized with an offset between 1.5mm and 3mm do not show visible deterioration. They are cut with Electrical Discharge Machining (EDM) as parallelepiped of 18 mm * 4 mm * 8 mm (Figs. 5 and 6).

They are analyzed through X-ray tomography and thickness maps of the steels strips as a ZY view (such as indicated in Fig. 6) are realized thanks to it. X-ray tomography produces stacks of images of the samples realized. Each pixel of an image depicts the absorbance of a voxel of mater analyzed. The size of the voxel for each sample is presented in Table 5. Hence, a stack of image represents a 3D view of the absorbance of a sample.

To produce the thickness maps of the strips, these images are treated on the Fiji software following the process depicted in Figure 7. They are first cropped and reoriented, then coded on 8 bits. It means that each pixel of each picture takes a value between 0 and 255. Pixels with high values (i.e. high absorbance values) are considered as steel, pixels with low values are not steel (aluminum alloy or void). The threshold between these values is selected to isolate the steel strip and minimize artefacts produced by the steel strip. It means that values below the threshold are set to 0 and the values above the threshold are set to 1. The border of the steel is often badly delimited, indeed the values of the area of aluminum alloy near the steel strip are artificially increase and hidden by the steel strip. This kind of artefacts are well documented [26].

Table 3. Welding parameters selected.

Synergic law	WFS (m/min)	TS (m/min)	WFS / TS	Preheat temperature (°C)	EP/EN (+/−)	Gas flow (L/min)
CMT-PADV 1369	8.3	0.9	9.2	150	3	14

Table 4. Energetic and dimensional properties of the bead produced with the selected welding parameters.

Width W (mm)	Height H (mm)	(W/H)	Wetting angle (°)	Heat input (J/mm)	Massic Energy (J/g)
6.51	2.56	2.54	103	120	4247

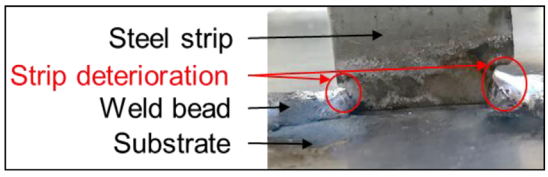

Fig. 3. Deterioration on the back of steels strip with offset < 1.5 mm.

Fig. 4. Steel strip not well bonded with the deposited bead for offset > 3.0 mm.

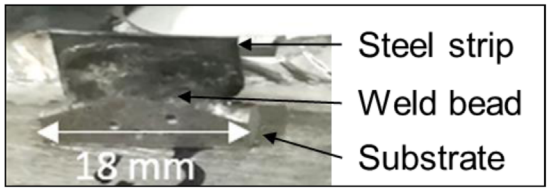

Fig. 5. Samples extracted.

These images are next stacked (added together) to produce an image representing a thickness map of the strip. Each pixel takes a value in number of voxels representing the thickness of the steel strip. These numbers are then converted into thickness values in millimeters thanks to the known voxel size.

As the nominal steel strip thickness is 0.55 mm, values above a threshold of 0.6 mm are considered as artifacts such as steel diluted in the aluminum alloy and are shown as black pixels.

The thickness maps produced of the steel strip are presented (Figs. 8–11). The color scale is presented in Figure 12. The area in yellow and red indicate severe deterioration (Refer to the online version of this article for full color figure).

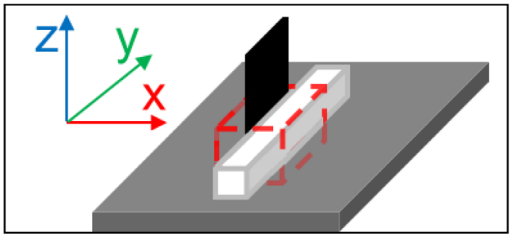

Fig. 6. Samples extraction (steel strip in black, substrate in gray, deposited bead in white).

Table 5. Voxel size for each sample.

Offset (mm)	1.5	2	2.5	3
Voxel size (μm)	10.53	11.00	11.54	10.51

The bonding of the strips with the deposited bead is analyzed on the samples realized with 2.5 mm and 3 mm. Some image produced by tomography following an XZ view (Fig. 13) can show voids area between the bead and the strip. These voids are not present on the sample realized with a 2.5 mm offset. The sample realized with a 3 mm offset is, hence, discarded and the one realized with a 2.5 mm offset is further analyzed.

The bonding quality of the sample realized with a 2.5 mm offset is analyzed through Scan Electron Microscopy (SEM).

The central part of this sample is isolated in Figure 14. It is then polished from steel side to aluminum alloy side only. No polishing is done from the aluminum alloy side toward the steel side so as to avoid spreading of aluminum alloy over steel (Fig. 15). The interface between the steel strip and the aluminum alloy bead is then inspected with SEM through back scatter diffraction (BSD) analysis following parameters presented in Table 6.

SEM show heavy elements brighter than light elements. It shows a bimetallic layer between aluminum alloy and steel. This bimetallic layer presents a width of 10 μm where it is the largest (Fig. 16).

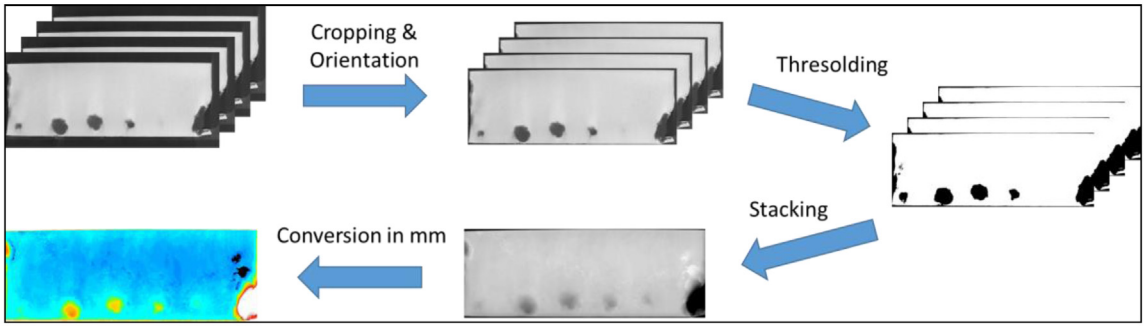

Fig. 7. Strip thickness map creation process.

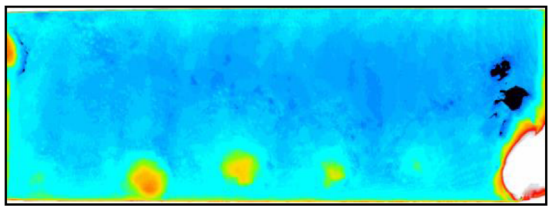

Fig. 8. Strip thickness map (offset = 1.5 mm).

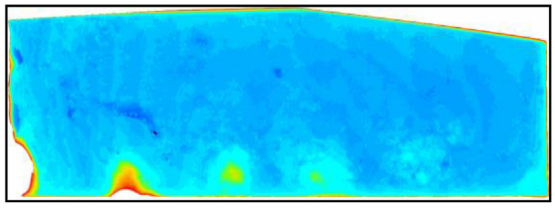

Fig. 9. Strip thickness map (offset = 2.0 mm).

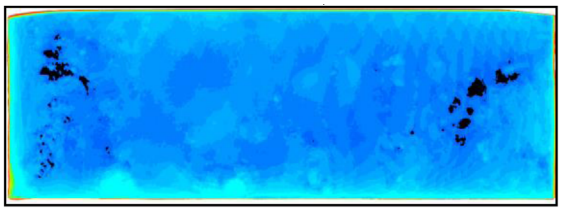

Fig. 10. Strip thickness map (offset = 2.5 mm).

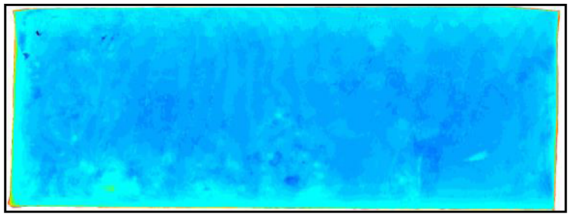

Fig. 11. Strip thickness map (offset = 3.0 mm).

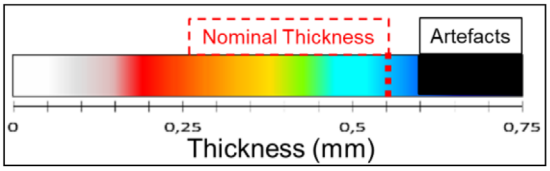

Fig. 12. Thickness map scale

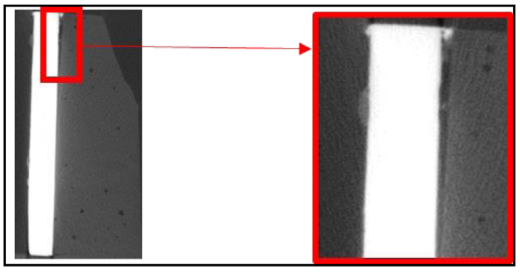

Fig. 13. XZ view of the sample realized with an offset of 3.0 mm (no material (black) between the steel strip (in white) and the aluminum alloy bead (in gray)).

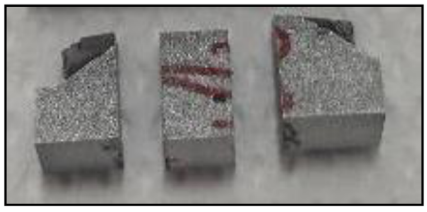

Fig. 14. Middle of the sample realized with a 2.5 mm offset isolated for SEM inspection.

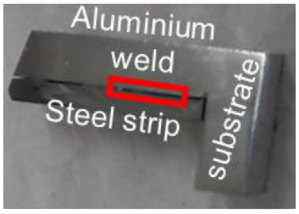

Fig. 15. Samples prepared for SEM inspection with the area inspected identified in red.

Table 6. SEM parameters.

Magnifying power	Signal type	Electron high tension (KV)	Working distance (mm)	Aperture number	Aperture size (μm)	High current
1500	BSD	10.00	8.1	4	60.00	On

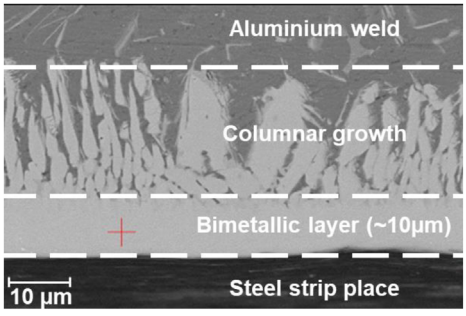

Fig. 16. View of the steel-aluminum alloy interface where it is the largest.

Fig. 18. Steel strip completely inserted between several layers.

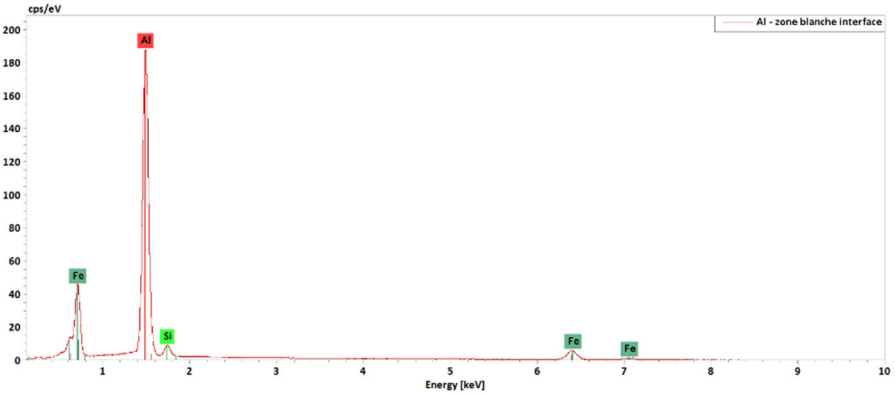

Fig. 17. EDS analysis on the point identified in Figure 16.

An EDS analysis on this layer show iron and aluminum atoms in a proportion distinctive of FeAl3 compound (Fig. 17). Indeed, the area below the aluminum peak is three times more important than the area below the iron peaks on this graph.

5 Discussion

Thickness maps of samples realized with an offset of 1.5 mm and 2.0 mm show severe deteriorations. These deteriorations are evenly distanced and can be explained by the CMT-PADV welding characteristics. Indeed, this kind of welding use pulse periodic welding.

It can be concluded that welding with an offset equal or inferior to 2.0 mm leads to a deterioration of the steel strip and is thus non-suitable to create a qualitative bonding.

It has been shown by observing a side view of the samples that an offset of 3.0 mm can lead to a bead and a strip separated by significant void space. It can be concluded that they are not well bonded together. Hence, observing an offset of 3.0 mm or more seems not suitable to embed a steel strip.

The bonding interface of the sample realized with an offset of 2.5 mm has been observed through SEM. A bimetallic layer has been identified with an EDS analysis. FeAl3 has been identified which is expected by literature [17,18]. This bimetallic layer presents a maximum thickness of 10 μm. This is a sign of a strong bonding according to literature [19].

Further work could be done to optimize process parameters such as the offset, to increase the strength and the quality of the bonding layer. The aim of the paper was to show the feasibility of a sound steel strip insertion during massive aluminum alloy part manufacturing. This has been assessed with the sample realized with an offset of 2.5 mm. The thickness maps realized by tomography and the SEM analysis of the interface presented in this paper are proofs of it. Moreover, the difference in thickness between the two

entities represents a ratio of 10, which is 3 times bigger than the previous work reported in the literature. An insertion of a steel strip below several layer has been successfully achieved with the parameters selected thanks to this study as shown in Figure 18.

6 Conclusion and perspectives

In this paper, a study presenting a configuration to embed a thin steel strip inside a massive aluminum alloy part made with WAAM is detailed. Samples realized with different steel strip − welding torch offset distances are produced. Their deterioration is evaluated through thickness maps realized with X-ray tomography. The bimetallic interface layer between the steel-strip and the aluminum alloy is analyzed through SEM and EDS to evaluate the bonding quality.

This study shows the feasibility of steel strip insertion during massive aluminum alloy part manufacturing with WAAM process. It is hence a step toward realization of smart metallic part and their state of stress control through a probe recording the magnetic signature of a magnetostrictive steel strip embedded inside it.

Next steps to achieve this goal are:

- To setup tensile tests to measure the strength of the bonding obtained upon shear and normal stress and thus to ensure the bonding quality on completely embedded samples such as the one presented in Figure 18.
- To characterize the magnetostrictive answer of the bimaterial part realized.
- To develop a methodology and tools that can be used in the smart product design phase to position the steel strip inside the host part in order to measure accurately the maximum load without damaging the host part.

These works are of great interest for the upcoming of smart metallic part, which is an important step toward industry 4.0.

Funding

Authors of this paper want to thank the AuRA region (French administrative region) for their funding of these studies.

References

[1] G.G. Meyer, K. Främling, J. Holmström, Intelligent products: a survey, Comput. Ind. **60**, 137–148 (2009)
[2] S.A. Rijsdijk, E.J. Hultink, How today's consumers perceive tomorrow's smart products, J. Prod. Innov. Manag. **26**, 24–42 (2009)
[3] M.E. Porter, J.E. Heppelmann, How smart, connected products are transforming companies, Harv. Bus. Rev. (2015). Available: https://hbr.org/2015/10/how-smart-connected-products-are-transforming-companies (accessed 22 July 2020)
[4] E.S. Gorkunov, S.M. Zadvorkin, S.V. Smirnov, S. Yu. Mitropol'skaya, D.I. Vichuzhanin, Correlation between the stress-strain state parameters and magnetic characteristics of carbon steels, Phys. Met. Metallogr. **103**, 311–316 (2007)
[5] T. Ricart, P. Robert, S. Basrour, N. Beraud, M. Museau, H. Paris, Method for determining a deformation of an area of a part obtained by additive manufacturing, WO/2023/281201 (2023). Available: https://www.sumobrain.com/patents/wipo/Method-determining-deformation-area-part/WO2023281201A1.html
[6] S.W. Williams, F. Martina, A.C. Addison, J. Ding, G. Pardal, P. Colegrove, Wire + arc additive manufacturing, Mater. Sci. Technol. **32**, 641–647 (2016)
[7] B. Vayre, F. Vignat, F. Villeneuve, Metallic additive manufacturing: state-of-the-art review and prospects, Mech. Ind. **13**, 89–96 (2012)
[8] K.E.K. Vimal, M. Naveen Srinivas, S. Rajak, Wire arc additive manufacturing of aluminium alloys: a review, Mater. Today: Proc. (2020)
[9] F.R. Teixeira, F.M. Scotti, R.P. Reis, A. Scotti, Effect of the CMT advanced process combined with an active cooling technique on macro and microstructural aspects of aluminum WAAM, Rapid Prototyp. J. **27**, 1206–1219 (2021)
[10] R. Li, H. Zhang, F. Dai, C. Huang, G. Wang, End lateral extension path strategy for intersection in wire and arc additive manufactured 2319 aluminum alloy, Rapid Prototyp. J. **26**, 360–369 (2019)
[11] N. Béraud, A. Chergui, M. Limousin, F. Villeneuve, F. Vignat, An indicator of porosity through simulation of melt pool volume in aluminum wire arc additive manufacturing, Mech. Ind. **23**, 1 (2022)
[12] P. Wang, X. Chen, Q. Pan, B. Madigan, J. Long, Laser welding dissimilar materials of aluminum to steel: an overview, Int. J. Adv. Manuf. Technol. **87**, 3081–3090 (2016)
[13] J. Lin, N. Ma, Y. Lei, H. Murakawa, Shear strength of CMT brazed lap joints between aluminum and zinc-coated steel, J. Mater. Process. Technol. **213**, 1303–1310 (2013)
[14] A. Chabenat, Montage des pièces pour soudage à l'arc électrique, Techniques de l'ingénieur, Mécanique − Travail des matériaux, Assemblage, p. 14, 2000
[15] P. Young, How to Weld Thin Metal − Welding Headquarters, weldingheadquarters. com (2020). Available from https://weldingheadquarters.com/how-to-weld-thin-metal/ (accessed 18 January 2022)
[16] K. Furukawa, New CMT arc welding process − welding of steel to aluminium dissimilar metals and welding of super-thin aluminium sheets, Weld. Int. **20**, 440–445 (2006)
[17] L. Agudo et al., Intermetallic FexAly-phases in a steel/Al-alloy fusion weld, J. Mater. Sci. **42**, 4205–4214 (2007)
[18] J. Singh, K.S. Arora, D.K. Shukla, Dissimilar MIG-CMT weld-brazing of aluminium to steel: a review, J. Alloys Compd. **783**, 753–764 (2019)
[19] L.A. Jácome et al., Influence of filler composition on the microstructure and mechanical properties of steel—aluminum joints produced by metal arc joining, Adv. Eng. Mater. **11**, 350–358 (2009)
[20] Y. Shi, L. Shao, J. Huang, Y. Gu, Effects of Si and Mg elements on the microstructure of aluminum-steel joints produced by pulsed DE-GMA welding-brazing, Mater. Sci. Technol. **29**, 1118–1124 (2013)
[21] R. Cao, G. Yu, J.H. Chen, P.-C. Wang, Cold metal transfer joining aluminum alloys-to-galvanized mild steel, J. Mater. Process. Technol. **10**, 1753–1763 (2013)
[22] B. Cong, J. Ding, S. Williams, Effect of arc mode in cold metal transfer process on porosity of additively manufactured Al-6.3%Cu alloy, Int. J. Adv. Manuf. Technol. **76**, 1593–1606 (2015)

[23] Fronius, CMT Pulse Advanced for joining high-strength steels, fronius.com (2020). Available from https://www.fronius.com/en-gb/uk/welding-technology/world-of-welding/fronius-welding-processes/cmt-pulse-advanced (accessed 26 August 2022)

[24] P. Robert, M. Museau, H. Paris, Effect of temperature on the quality of welding beads deposited with CMT technology, in *2018 IEEE International Conference on Industrial Engineering and Engineering Management (IEEM)* (2018), pp. 680–684

[25] T. Kumar, D.V. Kiran, N. Arora, P.S. Kumar, Study of steel-aluminium joining under the influence of current waveforms using advanced CMT process variants, Mater. Manuf. **0**, 1–18 (2022)

[26] C. Thiery, Tomographie à rayons X, Techniques de l'ingénieur, Mesures – Analyses | Techniques d'analyse (2015). Available: https://www.techniques-ingenieur.fr/doi/10.51257/a/v3/p950 (accessed 03 Jaunary 2022)

Cite this article as: P. Robert, N. Beraud, M. Museau, M. Limousin, H. Paris, Toward steel strip insertion during wire arc additive manufacturing of aluminum alloy smart part, Mechanics & Industry **24**, 15 (2023)